Electronic Supplementary Material (ESI) for Nanoscale.

Supporting Information

Hollow Silica Sphere Colloidal Crystals: Insights into Calcination Dependent Thermal Transport

Pia Ruckdeschel,[1] Tobias W. Kemnitzer,[2] Fabian A. Nutz,[1] Jürgen Senker,[2] Markus Retsch[1,]*

[1]University of Bayreuth, Physical Chemistry 1, Universitätsstr. 30, 95447 Bayreuth

[2]University of Bayreuth, Inorganic Chemistry 3, Universitätsstr. 30, 95447 Bayreuth

[*] markus.retsch@uni-bayreuth.de

Table S1. Elemental analysis – N, C, O content in HSNP calcinated at different temperatures.

	N content [%]	C content [%]	O content [%]
HSNP-500	0.054	0.254	0.317
HSNP-650	0.021	0.067	0.106
HSNP-800	0.026	0.035	0.010
HSNP-950	0.025	0.069	0.002

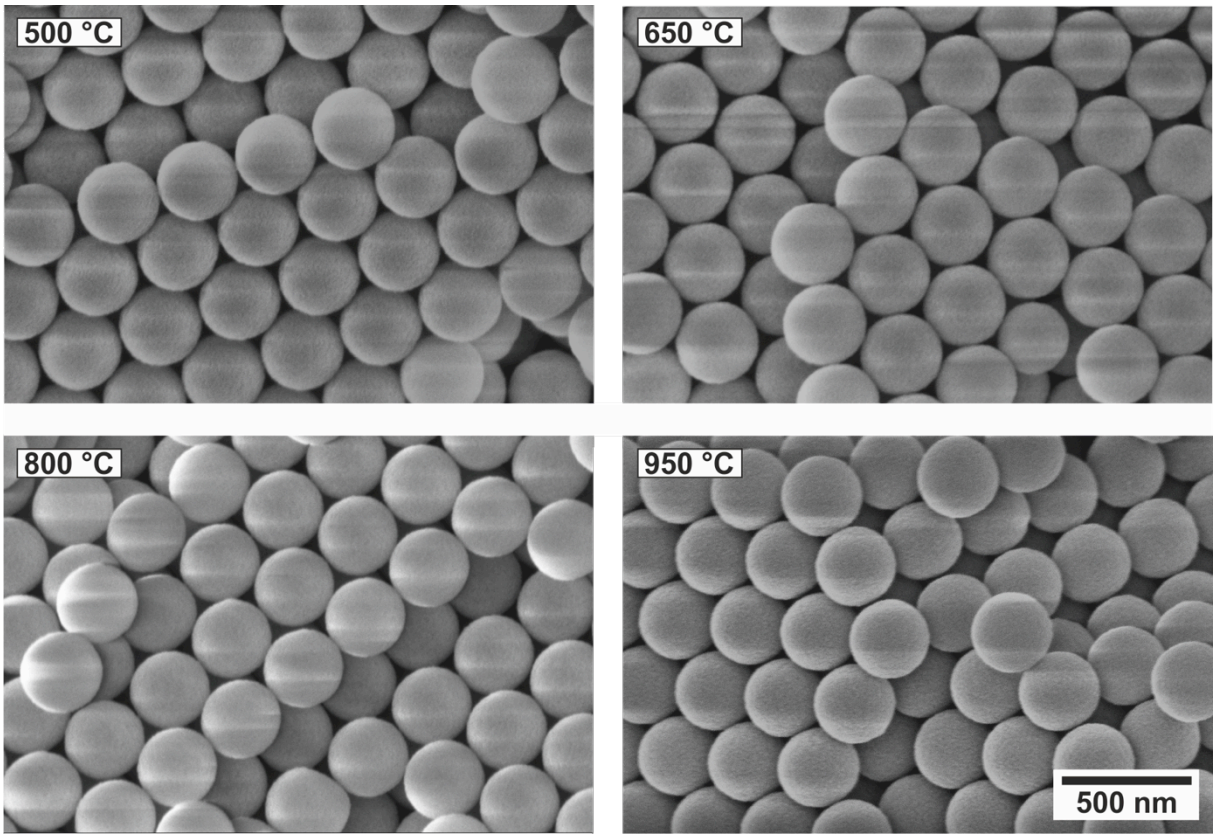

Figure S1. High magnification SEM images of HSNP calcinated at different temperatures (500 – 950 °C). No sinter necks between adjacent spheres can be observed, the particles retain their spherical shape and hexagonal assembly symmetry.

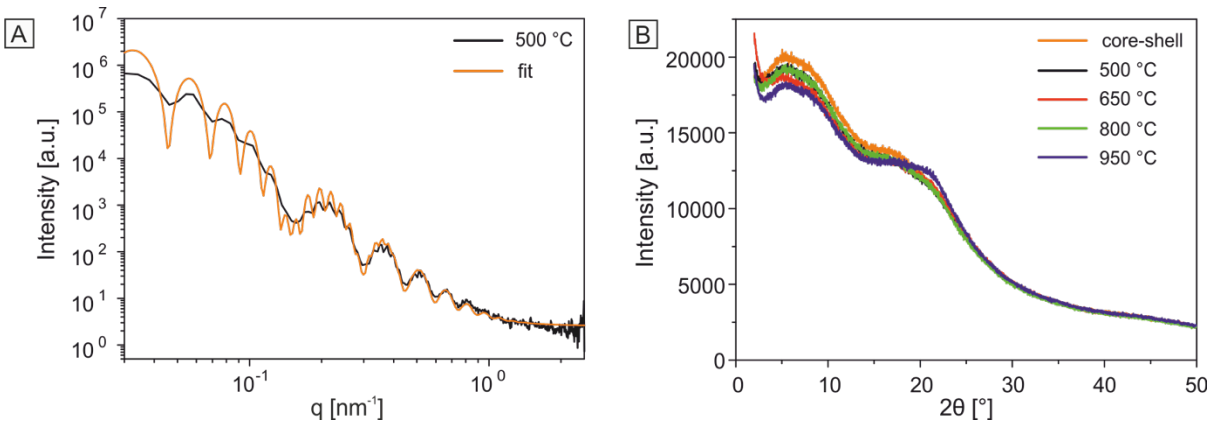

Figure S2. Internal structural characterization of HSNP. A) SAXS pattern for hollow silica nanoparticles calcinated at 500 °C: experimental scattering profile (black line) and the fitting curve (orange line). The fit parameters are 315 nm diameter and 42.5 nm shell thickness, B) XRD measurements of HSNP calcinated at different temperatures (500 – 950 °C).

Table S2. Summary of data received from NMR measurements.

	^{29}Si NMR [a]		***^{129}Xe NMR*** [c]	
	$Q^4/(Q^3+Q^4)$	**T_1 relaxation time [s]**	**Delta [ppm]**	**Cylindrical pore [nm]**
HSNP-500	0.88	33 ± 7 (20 ± 2)[b]	57, 105	1.11, 0.71
HSNP-650	0.92	96 ± 20	42, 105	1.42, 0.71
HSNP-800	0.94	272 ± 60	-	-
HSNP-950	0.94	6400 ± 1000	-	-

[a] Relative amount of Q^4 units and spin-lattice relaxation times obtained from solid state ^{29}Si NMR, [b] Spin-lattice relaxation time of HSNP-500 after drying to remove water residues, [c] Limiting shift of ^{129}Xe and corresponding pore sizes according to the Fraissard model for cylindrical pore geometries.

$$D(\partial) = \frac{243 \cdot 2.054}{\delta} - 2.054 + D_{Xe}$$

δ = Limiting shift, D_{Xe} = VdW-Diameter of Xe

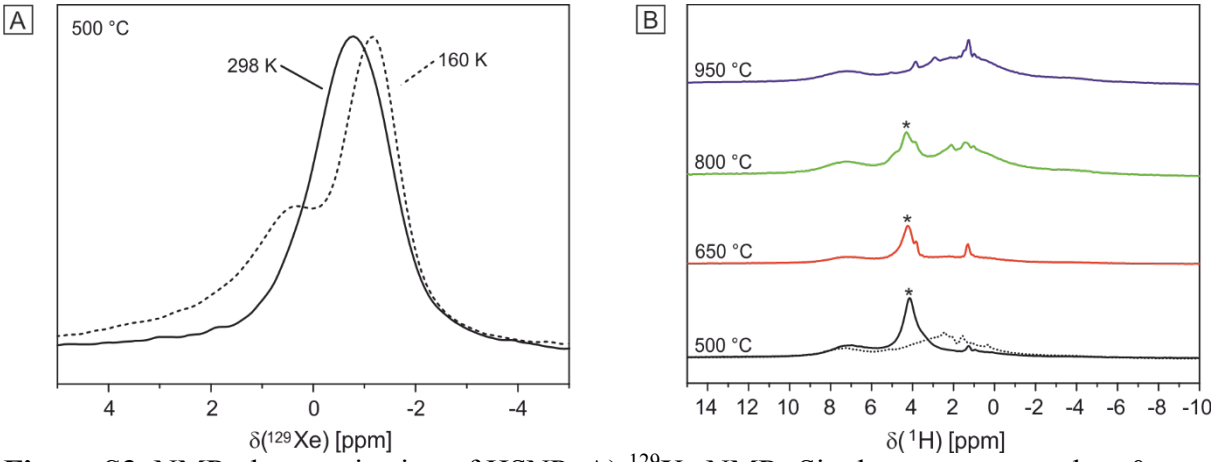

Figure S3. NMR characterization of HSNP. A) ^{129}Xe NMR: Single xenon gas peak at 0 ppm of silica hollow spheres at a measurement temperature of 298 K and 160 K, B) ^{1}H NMR spectra of silica hollow spheres calcinated at different temperatures (500 – 950 °C). The dotted line shows a pre-dried sample. The stars mark the peak caused by adsorbed water.

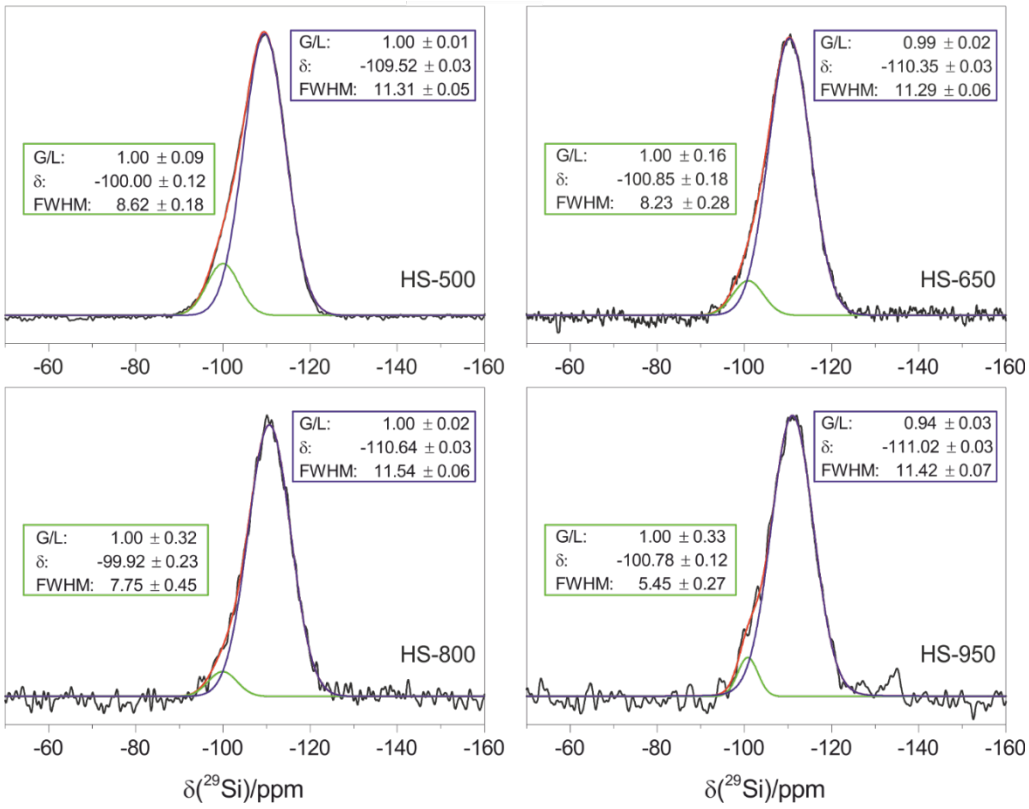

Figure S4. Deconvoluted projection of the ^{29}Si spectra of HSNP calcinated at 500 – 950 °C; measured signal (black), cumulative fit (red), simulated signals (green, blue).

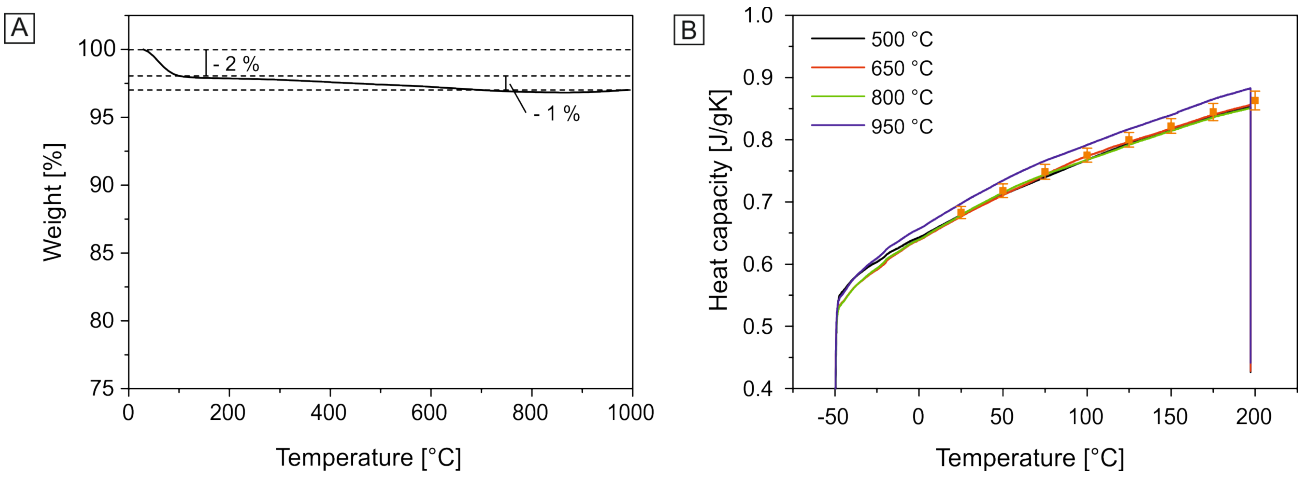

Figure S5. A) Thermogravimetric analysis (TGA) results of silica hollow spheres calcinated at 500 °C. The weight loss step (~ 2 %) at temperature up to 100 °C relates to the loss of adsorbed water. Another 1 % of mass is lost up to 950 °C, which can be attributed to the removal of trace amounts of silica condensation products. B) Differential scanning calorimetry (DSC) measurements of the compacted silica hollow spheres calcinated at 500 - 950 °C and the corresponding mean values (orange dots).

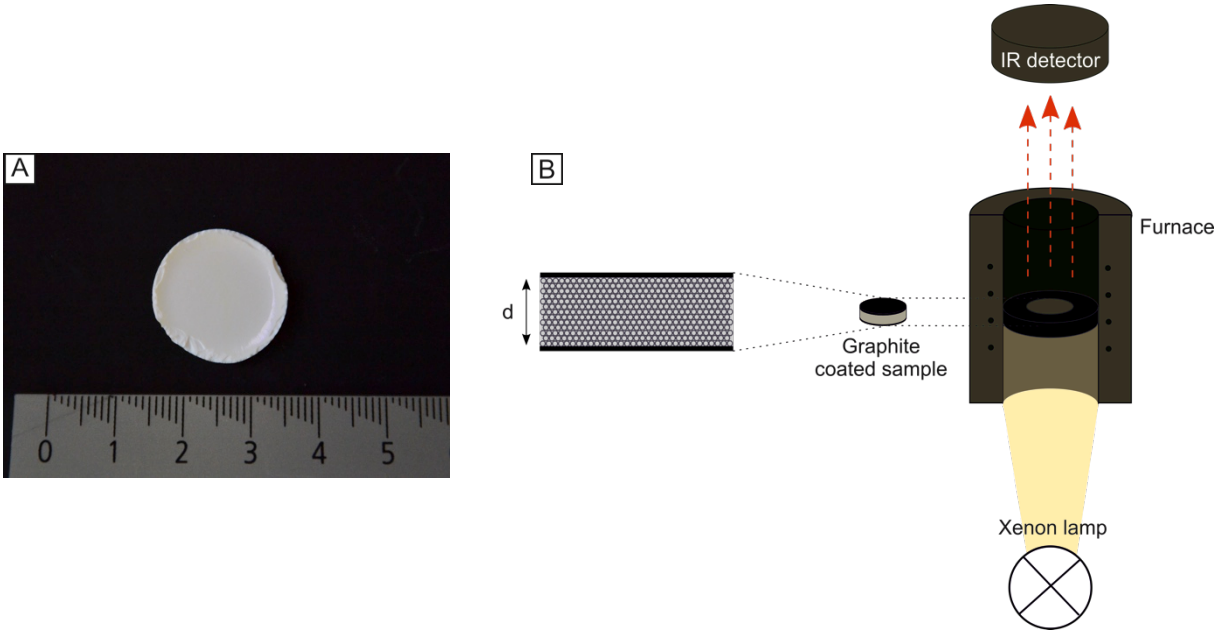

Figure S6. A) Photograph of a silica hollow sphere colloidal crystal with a diameter of 2 cm, B) LFA measurement principle and sample setup.

In brief, the colloidal crystals were coated on the top and bottom side with a thin graphitic layer (< 20 µm). Using a short light flash from a Xe white light source (2 ms) the bottom side of the sample is subjected to a temperature increase. The absorbed heat diffuses through the sample and consequently heats the top surface. An IR detector measures this time-dependent temperature increase. Using a radiation fit model the thermal diffusivity of the hollow sphere colloidal crystal sample can be extracted.

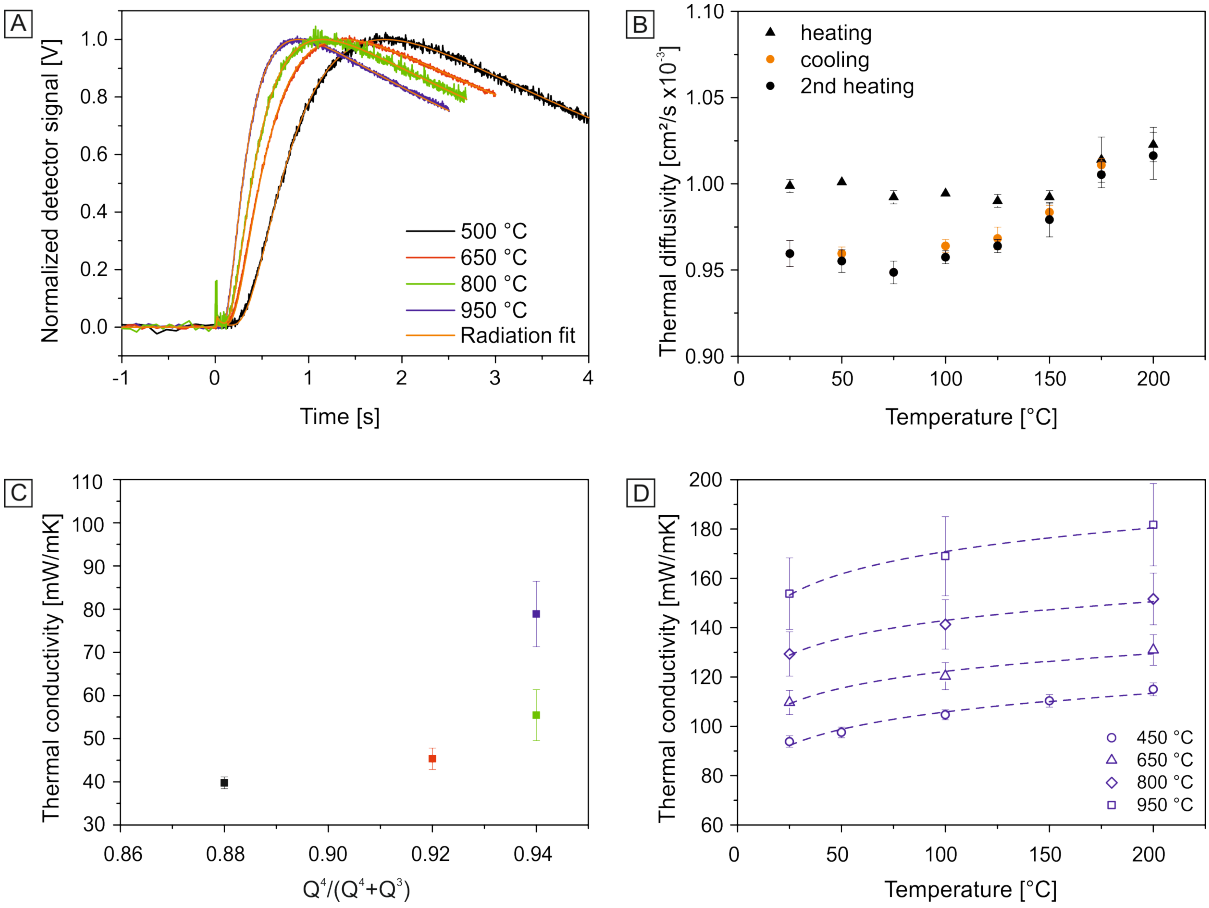

Figure S7. Laser flash analysis (LFA) of silica hollow sphere colloidal crystals A) Examples of LFA measurement signals of HSNP monoliths after calcination at elevated temperatures and the corresponding radiations fits (orange lines). The raw data were normalized to (0,1). Sample thicknesses were: 500 °C: 812 µm, 650 °C: 686 µm, 800 °C: 654 µm, 950 °C: 665 µm. B) Thermal diffusivity as a function of temperature of a HSNP colloidal crystal calcinated at 500 °C with heating (black) and cooling cycles (orange). C)Thermal conductivity of HSNP crystals calcinated at different temperatures in dependence of the degree of condensation, D)Thermal conductivity of annealed colloidal crystals (450 – 950 °C), calcinated at 950 °C prior to the assembly of the monoliths. The dashed lines represent $\kappa \sim T^x$.

The radiation fit model represents an expansion to the finite-pulse and heat-loss corrections implemented in the Combined fit model from Dusza (L. Dusza, High Temperatures - High Pressures, 1995, 27, 467-473). It accounts for a portion of the Xe flash to be directly transmitted to the top surface, leading to an instantaneous temperature jump analogous to Blumm *et al.*.(J. Blumm, J. Henderson, O. Nilsson and J. Fricke, High Temperatures-High Pressures, 1997, 29, 555-560).

Uncertainty analysis of the thermal conductivity determination

In the following, the uncertainty analysis of an individual sample based on independent measurements for the 500 °C calcinated HSNP colloidal crystal is shown exemplarily. The different contributions will be introduced separately:

Thermal conductivity κ:

$$\kappa = \alpha \cdot c_p \cdot \rho = \left(\frac{0.138 \cdot d^2}{t_{\frac{1}{2}}}\right) \cdot c_p \cdot \left(\frac{(r^3 - (r-t)^3) \cdot \rho_{SiO_2}}{r^3}\right)$$

Thermal diffusivity determination: $\alpha = \frac{0.138 \cdot d^2}{t_{\frac{1}{2}}}$

$$\sigma_\alpha = \sqrt{\left(\frac{\sigma\alpha}{\sigma t_{\frac{1}{2}}}\right)^2 \cdot \sigma_{t_{\frac{1}{2}}}^2 + \left(\frac{\sigma\alpha}{\sigma d}\right)^2 \cdot \sigma_d^2} = \left(-\frac{0.138 \cdot d^2}{\left(t_{\frac{1}{2}}\right)^2}\right)^2 \cdot \sigma_{t_{\frac{1}{2}}}^2 + \left(\frac{2 \cdot 0.138 \cdot d}{t_{\frac{1}{2}}}\right)^2 \cdot \sigma_d^2$$

Measured parameters and their standard deviation:

Half-rise time $t_{1/2}$: (0.926 ± 0.009) s

Layer thickness d: (812 ± 8) µm

Average thermal diffusivity and standard deviation:

α= (9.83 ± 0.22) ·10^{-8} m²/s

i) Heat capacity c_p determination: $\sigma_{c_p} = \sqrt{\frac{\sum(x-\bar{x})^2}{n-1}}$

Average c_p and standard deviation:

c_p: (0.683 ± 0.010) J/gK

ii) Particle density ρ determination: $\rho = \left(\frac{(r^3-(r-t)^3) \cdot \rho_{SiO_2}}{r^3}\right)$

$$\sigma_\rho = \sqrt{\begin{array}{c}\left(\frac{\sigma\rho}{\sigma r}\right)^2 \cdot \sigma_r^2 + \left(\frac{\sigma\rho}{\sigma t}\right)^2 \cdot \sigma_t^2 + \left(\frac{\sigma\rho}{\sigma\rho_{SiO2}}\right)^2 \cdot \sigma_{\rho_{SiO_2}}^2 = \\ (-3 \cdot \mathrm{t}(\mathrm{t}-\mathrm{r})^2 \cdot \frac{\rho}{r^4})^2 \cdot \sigma_r^2 + (3 \cdot (\mathrm{r}-\mathrm{t})^2 \cdot \frac{\rho}{r^3})^2 \cdot \sigma_t^2 + \left(\frac{(r^3-(r-t)^3)}{r^3}\right)^2 \cdot \sigma_{\rho_{SiO_2}}^2\end{array}}$$

Measured parameters and their standard deviation:

Shell thickness t: (43.7 ± 1.6) nm

Particle radius r: (157.9 ± 1.9) nm

Density of the shell by He pycnometry ρ_{SiO2}: (2.27 ± 0.13) g/cm³

Average density and standard deviation:

ρ= (1.044 ± 0.089) g/cm³

Calculation of the thermal conductivity κ:

$$\kappa = \alpha \cdot c_p \cdot \rho$$

Standard deviation of κ:

$$\sigma_\kappa = \sqrt{\left(\frac{\sigma\kappa}{\sigma\alpha}\right)^2 \cdot \sigma_\alpha^2 + \left(\frac{\sigma\kappa}{\sigma c_p}\right)^2 \cdot \sigma_{c_p}^2 + \left(\frac{\sigma\kappa}{\sigma\rho}\right)^2 \cdot \sigma_\rho^2}$$

Average thermal conductivity and standard deviation:

κ= (70.1 ± 6.3) mW/mK

We determined the standard deviation for each calcination dependent thermal conductivity measurement of our samples and confirmed that the relative error is < 10 % for most of the cases. The highest uncertainty was found to be 13 %.

We therefore conclude that the major source of uncertainty is given by variations from sample to sample. This is the data and uncertainty that we present in our manuscript, which is based on at least three independent samples at each calcination temperature.

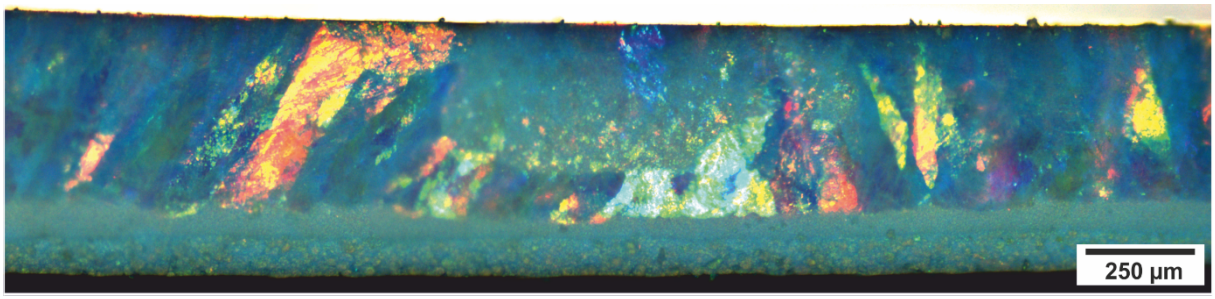

Figure S8. Bright field microscopy image of a colloidal crystal consisting of HSNP calcinated prior to the assembly process (annealed colloidal crystal).